A Computational Fluid Dynamic Modeling Study of Slag Fuming in Top Submerged Lance Smelting Furnace

Nazmul Huda, J. Naser, G. Brooks, M. A. Reuter, R. W. Matusewicz

Abstract—**Slag fuming is a process of extracting zinc from molten slag in the form of metal vapor by injecting or adding a reducing source such as pulverized or lump coal, natural gas, etc. Top Submerged Lance (TSL) technology has been successfully applied to extract zinc by a fuming process from residues from the zinc industry, ISF and QSL slag and Lead blast furnace slag. A Computational Fluid Dynamic model has been developed for zinc slag fuming process from ISF slag to investigate details of fluid flow and heat transfer in the furnace. The models integrate complex combustion phenomena and chemical reactions with the heat, mass and momentum interfacial interaction between the phases present in the system. The model is based on 3-D Eulerian multiphase flow approach and it predicted the velocity and temperature field of the molten slag bath and side wall heat fluxes. The model also predicted the mass fractions of slag and gaseous components inside the furnace. The model confirmed that rate of zinc fuming increases with temperature and is broadly consistent with experimental data.**

Index Terms— **Slag fuming, CFD, Top Submerged Lance, Zinc, Multiphase.**

I. Introduction

Primary production of zinc and lead produces slag or residues, which can contain significant amounts of zinc. The zinc content in these depends largely on the type of concentrate and residue materials, method of extraction and equipment used. Slag fuming is basically a secondary operation which is an important unit operation in the extraction of non-ferrous metals. Slag fuming has been used since 1930s to recover zinc from lead blast furnace slag [1]. It is mostly a batch process, in which a reducing mixture of air and pulverized coal is injected into the molten slag together with lump coal, however, Korea Zinc also fume in continuously operating furnaces. The coal-air mixture reduces the zinc oxide from the slag to metallic zinc vapor.

Zinc Fuming

Manuscript received March 17, 2010. The authors would like to express their gratitude to the Faculty of Engineering and Industrial Science, Swinburne University of Technology and Ausmelt Limited, for financial and technical support.

Nazmul Huda, PhD student, J. Naser, Senior Lecturer, G. Brooks, Professor, are with Swinburne University of Technology, Hawthorn, VIC 3122, Melbourne, Australia (Contact e-mail: Mhuda@Swin.edu.au)

M. A. Reuter, Chief Executive Technologist and R. W. Matusewicz, Technical Development Manager, are with Ausmelt Limited, 12, Kitchen Rd, Melbourne, VIC 3175, Australia.

Zinc slag fuming is a reductive treatment to recover zinc from zinc containing slag. The earliest experimental work on zinc fuming was conducted in Australia by Sulphide Corporation at Cockle Creek between 1906 and 1920 [2]. The process has become operative since 1930's to recover zinc from lead blast furnace slag. Operating temperatures lie between 1423 and 1573 K. The overall reactions occurring in the bath are,

$$ZnO_{(slag)} + C \rightarrow Zn_{(g)} + CO_{(g)} \quad (1)$$

$$C + CO_2 = 2CO \quad (2)$$

$$ZnO_{(slag)} + CO_{(g)} \rightarrow Zn_{(g)} + CO_{2_{(g)}} \quad (3)$$

The overall chemical reaction in the bath is thought to be controlled by the supply of carbon to the slag-gas interface [2-4]. The main reaction (1) is endothermic and combustion of fuel in the bath supplies the necessary heat. The vaporized zinc oxidizes when it comes in contact with the air above the zinc bath. The zinc oxide fume is subsequently collected in the bag house. Fig. 1 shows the schematic diagram of the zinc slag fuming process in the case of Top Submerged Lance blowing.

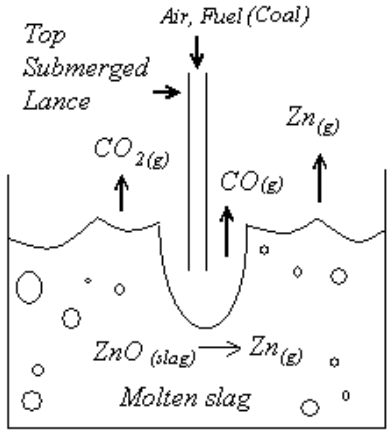

Fig. 1: Schematic diagram of slag fuming process from molten bath

II. Literature Review

Suzuki et al. [5] investigated the factors effecting the zinc fuming kinetics such as gas or slag composition, gas blow rate, slag temperature, viscosity and surface tension on a crucible scale experimental work. In their research, Suzuki et al. [5] found that formation of bubbles in the molten slag bath has a great influence on the zinc fuming kinetics. Richards et al. [2-4] carried out extensive research on kinetics of zinc slag-fuming process. In the first part of their research [2], they used industrial measurements to investigate the kinetic

ISBN: 978-988-18210-7-2
ISSN: 2078-0958 (Print); ISSN: 2078-0966 (Online)

phenomena in the zinc slag-fuming process. The industrial work consisted of slag sampling through the cycles of different fuming operations. They reported that the zinc reduction curve is linear with time and a portion of the injected coal entrains in the slag.

Later, Richards and Brimacombe [4] developed a mathematical model of zinc slag fuming based on a two reaction zones; (i) an oxidizing zone in the tuyere gas stream and a separate (ii) reduction zone at the gas slag interface. The authors reported that about 33% of the injected coal was entrained in the slag, 55% combusted in the tuyere gas column and 12% bypassed the bath completely. Richards and Brimacombe [3] elucidated the rate limiting steps of the fuming process and predicted the influence of process variables on fuming by using the two zone kinetic model [4]. The model predicts that fuming efficiency reaches maximum with increasing residence time of coal particles in the slag.

Cockcroft et al.[6] subsequently improved the model of Richards et al. [3] by further consideration of mass transfer, chemical kinetics and heat transfer in the system and also including the behavior of lead in the bath. Cockcroft et al. [7] reported that high pressure coal injection increased coal entrainment about 25%, from 65% for low pressure to 90% for high pressure. As a result fuming rates were increased substantially, to between 70% and 90%, depending on the charge mix. Richards [8] commented that coal entrainment is controlled by injection conditions whereas bath temperature is a function of coal combustion and ferrous oxide oxidation.

Further industrial studies have followed the studies by Richards et al. [2-4, 8, 9] and Cockcroft et al. [6, 7]. Miyake [10] described different aspects and optimized plant operating conditions of a slag fumer at the Hachinohe Smelter. Choi and Lee [11], Sofra et al. [12], Hughes et al. [13], Hoang et al. [14] described the Ausmelt's Top Submerged Lance (TSL) technology for the processing of secondary zinc feed materials, including zinc plant leach residues and EAF dust. More recently, the present authors [15] developed a CFD model for top submerged lance gas injection process, which they validated against an air-water system.

Although commercial slag fuming is well established, there have only been a few numerical modeling studies on zinc fuming kinetics. Kellogg [16] developed the first computer model for slag fuming process using programming language Fortran IV. In that model, Kellogg assumes stepwise equilibrium during each micro-step (0.1 minute in a 90 minute period). No CFD analysis has been found in the open literature regarding slag fuming. In this paper, we describe a model we have developed that includes combustion, reactions kinetics in CFD.

III. Computational Procedure

A 3D model of the Ausmelt pilot plant was developed using CAD. A schematic diagram of the model is shown in Fig. 2(a). The modeled furnace has a diameter of $D = 0.5$ m and length $Z = 1.68$ m. The modeled furnace was filled up to L=0.6 m with ISF slag of composition shown by point A in Fig. 3. A vertical lance with an annulus of inner diameter $d_i = 30$ mm and outer diameter $d_o = 42$ mm was fitted at the centre of the furnace. Air was injected through the annulus of the lance and CH_4 as fuel through the central hole into the slag bath. Necessary heat in the bath for smelting and reduction of the slag is supplied by combusting CH_4 at the lance tip.

A schematic diagram of the modeled furnace is shown on Fig. 2(a). Generated 3D course grid is shown in Fig. 2(b), fine grid is not shown here for visual clarity. The computational grid (283344 cells) used in the present study is too dense for visual presentation. All the cells in the calculation domain were polyhedral with a large number of hexahedral cells. As the computational domain consisted of hybrid unstructured meshes in curvilinear non-orthogonal coordinate system with Cartesian base vectors and refined regions in some locations, mentioning number of cells in each direction is complicated. The meshing procedure was carried out using the Fame Advanced Hybrid meshing technique [17].

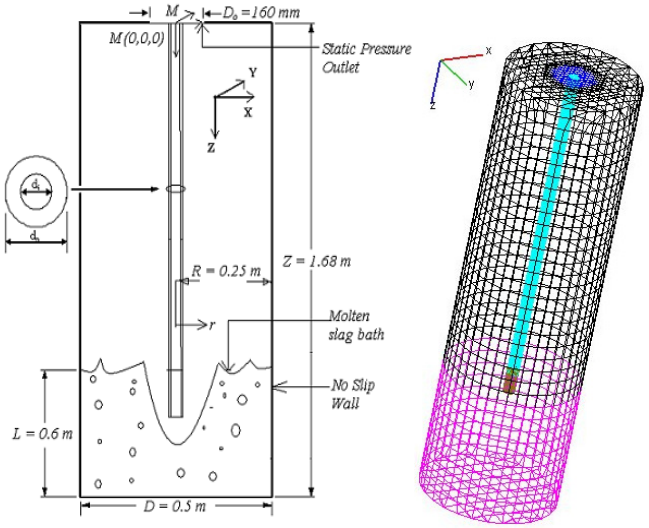

(a) (b)

Fig. 2: (a) Schematic diagram of the modeled furnace for Ausmelt's pilot plant trials, (b) Generated grid for CFD analysis

The multiphase flow simulation is based on Eulerian approach where gas and liquid phases interact with each other and there is significant exchange of momentum and energy between phases. In addition to mass and energy exchange between the constituents in each phase, there is also mass exchange between the gas and molten slag phase due to the phase transformation for chemical reaction in the slag bath. The model was developed by using commercial CFD package AVL FIRE 2008.2. Interfacial mass and energy exchange were modeled by using user-defined subroutines (UDF). The model developed include the following features,

1. Unsteady state multiphase solution for momentum and continuity.
2. Standard k-ε turbulence model for the turbulence modeling.
3. A cell centered finite volume approach was used to discretise the governing equations and the resulting discretised equations were solved iteratively using segregated approach.

ISBN: 978-988-18210-7-2
ISSN: 2078-0958 (Print); ISSN: 2078-0966 (Online)

4. Pressure and velocity were coupled using the SIMPLE algorithm [18].
5. For momentum and turbulence, first order upwind differencing scheme was used whereas central differencing scheme with second order accuracy was used for the continuity equation
6. All boundary conditions were chosen to match the flow condition of the pilot plant trials of the Ausmelt pilot plant.

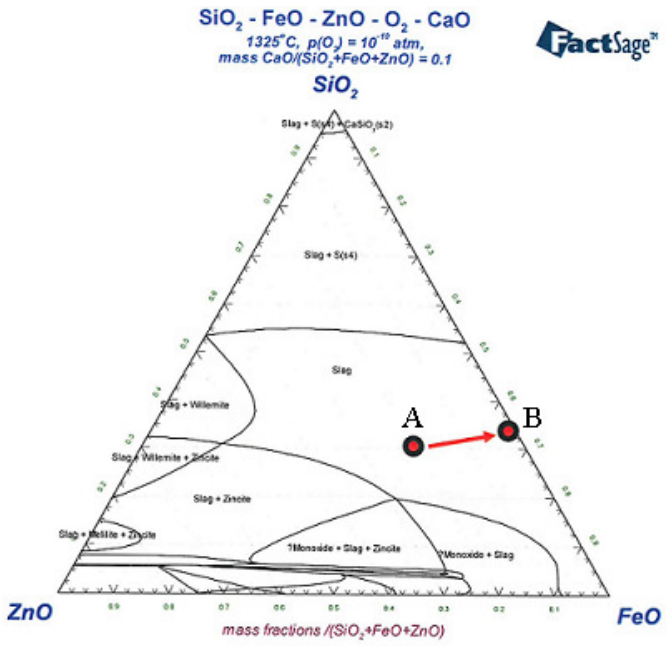

Fig. 3: Simplified phase relationships for the reduction step in an Ausmelt furnace for the components FeO_x, ZnO, CaO and SiO_2 generated by FACT Sage [19] for the given temperature, partial pressure as well as the lime content.

Basic Eulerian equations, describing multiphase combusting system are given by the conservation equations for continuity, momentum and enthalpy. Interfacial exchange terms for mass, momentum and energy in the gas-liquid interface is discussed below:

Interfacial Momentum Exchange

Momentum equation solved for the simulation can be expressed as,

$$\frac{\partial \alpha_k \rho_k v_k}{\partial t} + \nabla.\alpha_k \rho_k v_k v_k = -\alpha_k \nabla p + \nabla.\alpha_k \left(\tau_k + T_k^t\right) + \alpha_k \rho_k f + \sum_{l=1,l\neq k}^{N} M_{kl} + \sum_{l=1,l\neq k}^{N} \Gamma_{kl} \quad (4)$$

$\sum_{l=1,l\neq k}^{N} \Gamma_{kl}$ represents the interfacial mass exchange and $\sum_{l=1,l\neq k}^{N} M_{kl}$ represents the momentum interfacial interaction between phases k and l, f is the body force vector which comprises of gravity (g), p is pressure. Momentum interfacial exchange between gas and liquid has been modeled by implementing interfacial momentum source at the interface which includes drag and turbulent dispersion forces [17]:

$$M_c = C_D \frac{1}{8} \rho_c A_i''' |v_r| v_r + C_{TD} \rho_c k_c \nabla \alpha_d = -M_d \quad (5)$$

where c denotes continuous and d denotes the dispersed phase. The first term in equation (5) represents mean contributions due to drag force and the second term takes into account the turbulence effect. The turbulence effect is represented by a global dispersion effect, which is proportional to the void fraction gradient (cited in [20]).

The drag coefficient, C_D, is a function of the bubble Reynolds number, Re_b. The following correlation for drag coefficient, C_D, was used [17]:

$$C_D = \frac{24}{\mathrm{Re}_b}\left(1 + 0.15\,\mathrm{Re}_b^{0.687}\right) \qquad \mathrm{Re}_b \leq 1000 \quad (6)$$

Bubble Reynolds number, Re_b, and can be defined as:

$$\mathrm{Re}_b = \frac{v_r D_b}{\upsilon_c} \quad (7)$$

Where υ_c is the kinematic viscosity for continuous phase. Relative velocity is defined as:

$$\mathbf{v}_r = \mathbf{v}_d - \mathbf{v}_c$$

The interfacial area density for bubbly flow can be expressed as [17]:

$$A_i''' = \frac{6\alpha_d}{D_b} \quad (8)$$

where D_b = 0.1 mm is the bubble diameter and α_d is dispersed phase volume fraction. Bubble dispersion coefficient used in equation (5) was,

$$C_{TD} = 0.07$$

Combustion Modeling at the Lance Tip

For gas phase reaction, only one step CH_4 combustion reaction at the lance tip is considered as described by (9),

$$CH_4 + 2(O_2 + 3.76N_2) \rightarrow CO_2 + 2H_2O + 2\times 3.76N_2 \quad (9)$$

Species transport equation solved for gas phase reaction can be expressed as:

$$\frac{\partial}{\partial t}(\rho y_k) + \frac{\partial}{\partial x_i}\left(\rho(U_i - U_{\delta i}) y_k\right) = \frac{\partial}{\partial x_i}\left(\Gamma_{y_k}^{ii} \frac{\partial y_k}{\partial x_i}\right) + S_{y_k} \quad (10)$$

where y_k represents the mass fraction of an individual chemical species k. K_{gas} is the total number of chemical species. Γ_{y_k} can be defined as:

$$\Gamma_{y_k} = \left(\rho D_{k,m} + \frac{\mu_t}{Sc_t}\right) \quad (11)$$

where $D_{k,m}$ [m^2/s] is the diffusion coefficient for each species k in the mixture and $Sc_t = 0.7$ is the turbulent Schmidt number. The mass source S_{y_k} in the species transport equation is defined as,

ISBN: 978-988-18210-7-2
ISSN: 2078-0958 (Print); ISSN: 2078-0966 (Online)

$$S_{y_k} = \tilde{\omega}_{fu}.M_k.V_{Cell} \tag{12}$$

Where, $\tilde{\omega}_{fu}$ [kmol/(m^3/s)] is the reaction rate of species *k* and M_k [kmol/kg] is the molecular weight of species *k* and V_{cell} [m^3] is the volume of the computational cell. The rate of the reaction of species *k*, $\tilde{\omega}_{fu}$ [kmol/(m^3/s)] is calculated by the Eddy Break up combustion model [21].

$$\tilde{\omega}_{fu} = -\bar{\rho}\frac{\varepsilon}{k}\min\left[C_R\tilde{Y}_{fu}, C_R\frac{\tilde{Y}_{ox}}{s}, C_R'\frac{\tilde{Y}_{pr}}{1+s}\right] \tag{13}$$

Interfacial Energy Exchange:

Total enthalpy conservation equation solved for the model can be expressed as,

$$\frac{\partial\alpha_k\rho_k h_k}{\partial t} + \nabla.\alpha_k\rho_k v_k h_k = \nabla.\alpha_k(q_k + q_k^t) + \alpha_k\rho_k q_k''' + \nabla.\alpha_k\tau_k.v_k + \alpha_k\frac{\partial p}{\partial t} + \sum_{l=1,l\neq k}^{N} H_{kl} + h_k\sum_{l=1,l\neq k}^{N}\Gamma_{kl} \tag{14}$$

where q_k''' is the enthalpy volumetric source, heat flux, q_k, is defined as,

$$q_k = \frac{k_k}{c_{p,k}}\nabla h_k \tag{15}$$

where k_k is the phase *k* thermal conductivity, h_k is the phase *k* enthalpy. Turbulent heat flux, q_k^t, equals:

$$q_k^t = \frac{\mu_k^t}{\sigma_T}\nabla h_k \tag{16}$$

Γ_{kl} and H_{kl} in equation (14) represents mass and energy interfacial exchange between phases *k* and *l*. Heat generated due to the CH_4 combustion at the lance tip is transferred to the molten slag phase by considering interfacial energy exchange at the gas-liquid interface. Heat transfer between the two phases is modeled by using Ranz-Marshal enthalpy exchange model [17] as follows:

$$H_c = \frac{k_c}{D_b}Nu * A_i'''(T_d - T_c) = -H_d \tag{17}$$

where, k_c is the thermal conductivity of the molten slag phase, D_b is the bubble diameter and A_i''' is the interfacial area density defined as:

Nu is the Nusselt number and can be expressed as:

$$Nu = 2.0 + 0.6\,\mathrm{Re}_b^{\frac{1}{2}}\,\mathrm{Pr}^{\frac{1}{3}} \tag{18}$$

where, Re_b is the local bubble Reynolds number, and Pr is the Prandtl number.

Interfacial Mass Exchange

Interfacial mass exchange at the gas-liquid interface in the slag fuming process occur only due to the chemical reaction in the slag phase. Chemical species in the slag phase has been defined by a number of scalars and the following scalar equation has been solved for each scalar for slag phase reaction.

$$\frac{\partial}{\partial t}\alpha_k\rho_k\phi_{ki} + \nabla.\alpha_k\rho_k v_k\phi_{ki} = \nabla.\alpha_k\rho_k D_{ki}\nabla\phi_{ki} + S_{ki} \tag{19}$$

where S_{ki} is the source term for different scalars.

Phase transformation between molten slag and gas phase was considered by the following equation [17],

$$\Gamma_c = C_{mx}\alpha_c^{n1}\alpha_d^{n2}\rho_c = -\Gamma_d \tag{20}$$

Where, *c* and *d* denotes the continuous and dispersed phase, C_{mx} is the rate of phase transformation, ρ_c is the density for continuous phase, α is the volume fraction and volume fraction exponent used in the model are $n1 = 1$ and $n2 = 0$.

Fluid properties and initial condition

The flow was started with small initial values assigned to *k* and *ε*, which made the initial turbulent viscosity roughly equal to the kinematic viscosity for molten slag. For gas phase reaction given in equation (9), fluid and thermal properties of the different species involved in the solution process (density, specific heat, dynamic viscosity, molecular weight, thermal conductivity, diffusion coefficient) has been considered from the internal thermodynamic database of AVL FIRE [22]. The fluid and thermal properties for molten slag phase are mentioned in Table I.

Table I: Fluid and thermal properties of molten slag phase

Density (kg/m^3)	3500
Specific heat (J/kg K)	400
Dynamic viscosity (N s/m^2)	0.015
Thermal conductivity (W/m K)	10
Turbulent Prandtl number	0.5
Reference pressure (Pa)	100000
Reference temperature (K)	1500

Typical turbulence quantities at the inlet of the domain were calculated from inlet velocities by considering turbulence intensity $I = 0.05$ where, $I = u'/U_{inlet} \cong 0.16(\mathrm{Re})^{-1/8}$.

IV. Results and Discussions

Zinc fuming is a very complex process to simulate and it is necessary to make a number of assumptions to simplify the simulation. A large number of complex reactions are involved, such as: reduction of zinc oxide and ferric iron, fuel combustion, oxidation of ferrous iron oxide. In the present simulation, only reduction of zinc oxide and fuel combustion has been considered. We ignore the other reactions taking place in the system (the oxidation of Fe is likely to be important). Also, carbon was considered as a separate species assuming that 100% of the coal is fixed carbon with no volatile and ash content (which we know to be incorrect). As the numerical simulation is based on Eulerian approach, it doesn't show the exact plume shape with sharp gas-liquid interface (e.g. collapsing bubble plumes). However, the results here represent a significant step in developing a comprehensive model.

Temperature distribution for two separate phases is shown in Fig. 4. Fig. 4(a) shows the predicted temperature profile of the molten slag phase only after 30 seconds of the reduction stage. Because of the computational limitation, the simulation was run only for 30 seconds of real time. The present simulation only considers the reduction stage of the zinc fuming process. The simulation results revealed that there is

ISBN: 978-988-18210-7-2
ISSN: 2078-0958 (Print); ISSN: 2078-0966 (Online)

non-uniform temperature distribution in the molten slag bath. This temperature profile doesn't imply steady state distribution. These non-uniform temperature distributions in the slag bath are expected to be uniform with longer simulation time.

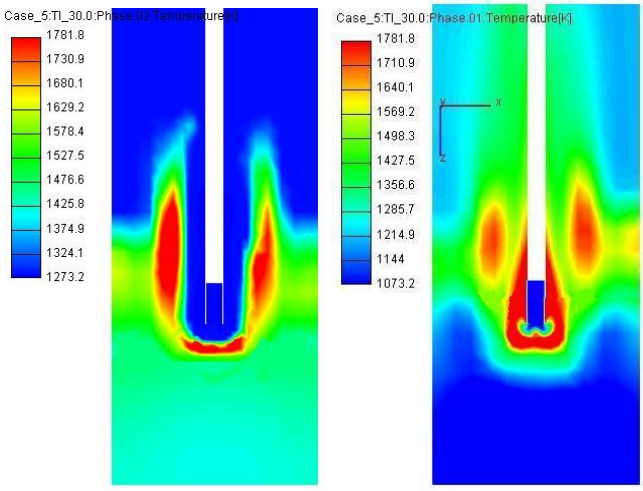

(a) (b)

Fig. 4: Temperature profile inside the furnace (a) molten slag only (b) gas phase only

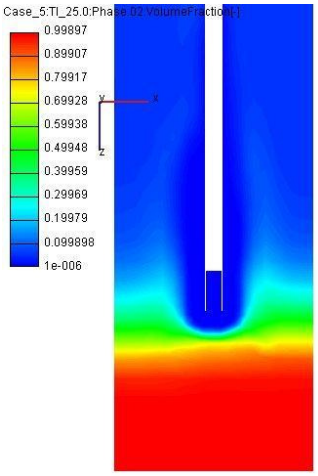

Fig. 5: Volume fraction distribution for molten slag phase only

From the simulation results, the molten slag bath can be divided into three zones: combustion zone near the lance tip (1680-1780 K), bath zone below the lance tip in the bath (1500-1600 K) and the bottom zone near the bottom surface of the furnace (1380-1430 K). Near the surface area of the molten slag bath, there was a thin layer of gas-liquid mixture. The transport properties of the molten slag phase influences this temperature distribution in the slag and the concentration of FeO (which we currently ignored) is likely to influence these properties significantly. Fig. 4(b) shows the temperature distribution for gaseous phase inside the furnace which shows the highest temperature distribution is at the lance tip and above the bath. Fig. 5 shows the volume fraction distribution for molten slag phase after 25 seconds of transient simulation. The sloshing and splashing phenomena above the slag bath is clearly visible from the volume fraction plot.

After the initiation of the combustion at the lance tip, the plume becomes larger because of the combustion and expansion of the gases in the slag bath. There is massive agitation in the slag bath and sloshing phenomena is observed from the simulation. The CFD software we used (AVL FIRE) enables us to capture results even for micro second. The simulation results predict that zinc fuming initiates from the near the surface area of the molten slag bath in the combustion zone where CO_2 forms as a product of combustion of CH_4. In the combustion zone, CO forms from the CO_2 by Boudouard reaction as mentioned in equation (2). CO thus formed initiates the first fuming process in the bath. Fig. 6(a) shows the initial stage zinc fuming process near the lance tip area. The fuming process accelerates from the bath near the surface area where the temperature rises rapidly and carbon reacts directly with ZnO in the molten slag. Fig. 6(b) shows the fumed zinc distribution inside the furnace from the molten slag bath.

Fig. 7(a) shows the species mass fraction distribution of CH_4 in the combustion chamber at the lance tip after 10.5 seconds of the simulation which shows CH_4 being almost combusted because of stoichiometric combustion. Because of the swirling effect in the annular region of the lance, O_2 in the air mixes well with the CH_4 in the combustion chamber and ensures fuel-efficient combustion at the lance tip. Formation of CO_2 in the bath is shown in Fig. 7(b). The present simulation was carried out on the assumption that the CO/CO_2 ratio is 1.

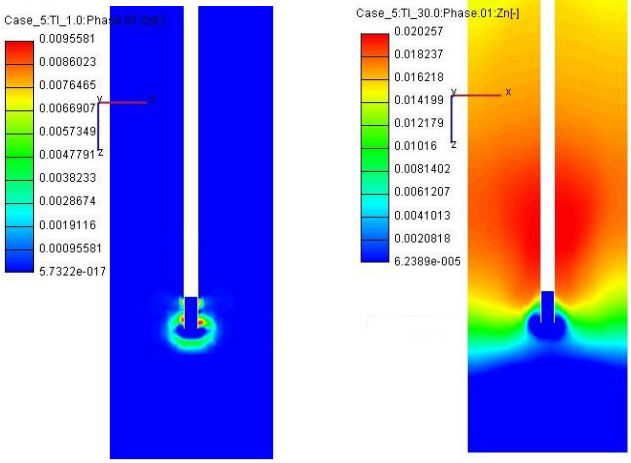

(a) (b)

Fig. 6: Fumed zinc distribution inside the furnace (a) at initial stage (b) after 30 seconds

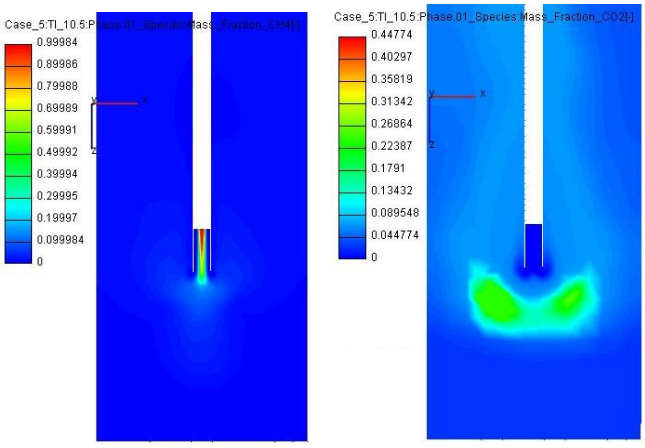

(a) (b)

Fig. 7: (a) Species mass fraction distribution for CH_4, (b) Species mass fraction distribution for CO_2

ISBN: 978-988-18210-7-2
ISSN: 2078-0958 (Print); ISSN: 2078-0966 (Online)

Fig. 8 shows the fuming rate of Zn from the bath as a function of temperature, experimental data are also shown for comparison. Experimental work was done by Waladan et. al [23] on crucible scale test work with ISF slag of 9.6% *ZnO*. The present simulation was carried out by considering ISF slag of 18% *ZnO* shown by point A in Fig. 3. Minor elements in the ISF slag were not taken into consideration for the present simulation. The produced curve shows the increasing fuming rate with temperature, which is also consistent with experimental results.

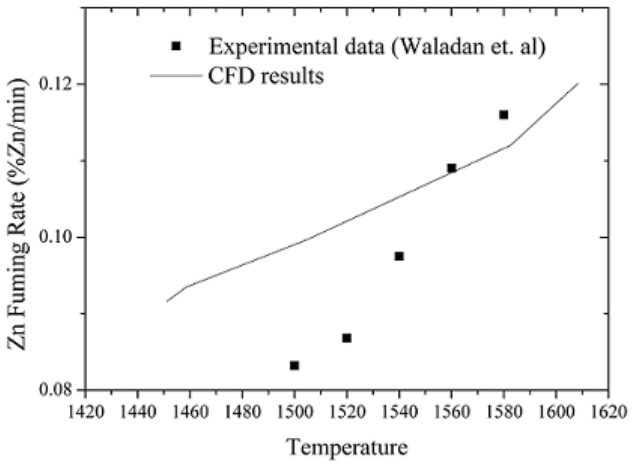

Fig. 8: Zinc fuming rate as a function of temperature and comparison with experimental results of Waladan et. al [23]

The simulation results showed zinc concentration in the slag decrease linearly with time. The linear time dependence of the zinc elimination rate reveals the zero order reaction kinetics, which is also consistent with the experimental results of Richards et. al [2]. Few improvement of the model, particularly, the treatment of the oxidation of Fe and providing a more realistic treatment of the behavior of coal will be incorporated. Even with these problems, these results appear very promising.

V. Conclusions

The simulation results give some interesting insights for complex metallurgical flows and transient concentrations of slag components and gaseous species inside the molten slag bath. These simulations reveal the zero order reaction kinetics of the zinc fuming process and suggest temperature distribution and plume shape in the molten slag bath for the 30 seconds of simulation. The results also showed that zinc elimination rate increases with temperature. The model is still in the improvement and validation phase. Detail reaction kinetics with all the elements of ISF slag will be incorporated to improve the model in addition to longer simulations. This model forms the basis in developing more complex models to help predict actual operations beyond simple flow modeling.

Acknowledgment

The authors would like to thank Mr. Brian Lightfoot for useful discussions.

References

1. Reddy, R.G., V.L. Prabhu, and D. Mantha, *Zinc Fuming from Lead Blast Furnace Slag*. High Temperature Materials and Processes, 2003. **21**(6): p. 377-386.
2. Richards, G.G., J.K. Brimacombe, and G.W. Toop, *Kinetics of Zinc Slag-Fuming Process: Part I. Industrial Measurements* Metallurgical and Materials Transaction B, 1985. **16**(B): p. 513-527.
3. Richards, G.G. and J.K. Brimacombe, *Kinetics of Zinc Slag-Fuming Process: Part III. Model Predictions and Analysis of Process Kinetics.* Metallurgical and Materials Transaction B, 1985. **16**(B): p. 541-549.
4. Richards, G.G. and J.K. Brimacombe, *Kinetics of Zinc Slag-Fuming Process: Part II. Mathematical Model.* Metallurgical and Materials Transaction B, 1985. **16**(3): p. 529-540.
5. Suzuki, R., S. Goto, and K. Azuma, *On Fuming of Zinciferrous Slags.* Journal of The Faculty of Engineering, University of Tokyo (B), 1970. **XXX**(3): p. 247-287.
6. Cockcroft, S.L., G.G. Richards, and J.K. Brimacombe, *Mathematical Model of Lead Behaviour in the Zinc Slag Fuming Process.* Canadian Metallurgical Quarterly, 1988. **27**(1): p. 27-40.
7. Cockcroft, S.L., G.G. Richards, and J.K. Brimacombe, *High Pressure coal injection in Zinc Slag Fuming.* Metallurgical and Materials Transaction B, 1989. **20**(B): p. 227-235.
8. Richards, G.G. *Optimization of the Zinc Slag Fuming Process*. in *EPD Congress*. 1994: TMS. 525-537.
9. Richards, G.G. *Continuous Fuming of Zinc - Containing Slags*. in *The Howard Worner International Symposium on Injection in Pyrometallurgy*. 1996. Melbourne, Australia: TMS. 97-105.
10. Miyake, M., *Zinc-Lead Smelting at Hachinohe Smelter*. 1995: Hachinohe p. 39-50.
11. Choi, C.Y. and Y.H. Lee, *Treament of Zinc residues by Ausmelt Technology at Onsan Zinc Refinery*, in *REWAS - Global Symposium on Recycling, Waste Treatment and Clean Technology*. 1999: San Sebastian, Spain.
12. Sofra, D.J. and A. Heinz. *Effective Treatment of Zinc Bearing Dusts & Residues – Solution Ausmelt Technology*. in *EMC*. 2003. Hannover, Germany. 491-506.
13. Hughes, S., R.W. Matusewicz, M.A. Reuter, and D. Sherrington. *Ausmelt- Extractive value from EAF Dust*. in *EMC* 2007. Dusseldorf, Germany. 1193-1208.
14. Hoang, J., M.A. Reuter, R. Matusewicz, and S. Hughes. *Top Submerged Lance (TSL) Direct Zinc Smelting*. in *Zinc Processing Conference*. 2008. Brisbane, Australia.
15. Huda, N., J. Naser, G. Brooks, M.A. Reuter, and R. Matusewicz, *CFD Modeling of Swirl and Non-swirl Gas Injections into Liquid Baths Using Top Submerged Lances* Metall. Trans. B., 2010. **41**(1): p. 35-50.
16. Kellogg, H.H., *A Computer Model of the Slag-Fuming Process for Recovery of Zinc Oxide.* Transactions of the Metallurgical Society of AIME, 1967. **239**: p. 1439-1449.
17. *AVL FIRE CFD Multiphase Manual v 8.5*. 2008, Austria: AVL.
18. Patankar, S.V. and D.B. Spalding, *A Calculation Procedure for Heat, Mass and Momentum Transfer in Three-Dimensional Parabolic Flows* Int. J. Heat. Mass. Trans., 1972. **15**: p. 1787-1806.
19. BALE, C.W., et al., *Factsage thermochemical software and databases - recent development* Computer Coupling of Phase Diagram and Thermochemistry, 2008. **33**: p. 295-311.
20. Chahed, J., V. Roig, and L. Masbernat, *Eulerian-Eulerian two-fluid model for turbulent gas-liquid bubbly flows.* Int. J. Multiphase Flow, 2003. **29**: p. 23-49.
21. Magnussen, B.F. and B.H. Hjertager. *On Mathematical Modelling of Turbulent Combustion with Special Emphasis on Soot Formation and Combustion*. in *Proceedings of the 16th Symposium (International) on Combustion* 1976: The Combustion Institute. p. 719-729.
22. *AVL FIRE CFD Species Transport Manual V 8*. 2006, Austria: AVL.
23. Waladan, M., G.R. Firkin, J. Bultitude-Paull, B.W. Lightfoot, and J.M.Floyd, *Top Submerged Lancing for Recovery of Zinc from ISF Slag*, in *Lead-Zinc Conferrence' 90*. 1990: California, USA.